ELECTRON BEAM PROBE FOR ION BEAM DIAGNOSTICS.

V. SHESTAK[†], C.J. KOST, R. BURGE, D.B. STESKI[‡], AND S. KORNAK[*]

Abstract

The electron beam probe (EBP) is a low energy electron beam used for non-destructive ion beam diagnostics. The EBP uses the deflection of low energy electrons due to the fields of the ion beam to provide information about the charge distribution of the ion beam such as size, centroid, profile, and current of the ion beam. At present we are testing the theory to see the abilities of this system.

[†]Moscow Physical Engineering Institute, Dept. of Electrophysical Installations, U.S.S.R.
[‡]University of Manitoba
[*]University of British Columbia

Electron Beam Probe for Ion Beam Diagnostics

V. Shestak, C.J. Kost, R. Burge, D.B. Steski, and S. Kornak

September 30, 1987

Contents

List of Figures

1 INTRODUCTION

Table 1
NON-INTERSECTING DIAGNOSTIC METHODS

METHOD (Monitors)	Measured Beam Parameters												REFERENCES
	NEUTRALIZATION	Current		Profile		SIZE	POSITION	SYMMETRY	TIME STRUCTURE	ENERGY	COMMENTS		
		PULSED	DC	TRANSVERSE	LONGITUDINAL								
Beam Transformers		x	x				x		x				1
Residual Gas Ionization		x	x	x		x	x	x			Pressure Dependent		2
Pickup Electrodes		x			x				x	x			3
Cavity Monitors		x			x		x		x	x			4
Synchrotron Radiation		x	x	x	x	x	x	x	x	x	High Energy Beams		5
Laser Systems	x	x	x	x	x	x	x	x	x	x	High Current Beams		6
Emitted Light		x	x	x		x	x	x					7
Emissive Probe	x	x	x	x		x	x	x					8
Electron Beam Probe	x	x	x	x	x	x	x	x	x	x			9

The electron beam probe (EBP) is a low energy electron beam used for non-destructive ion beam diagnostics.There are many well known methods of non-destructive ion beam diagnostics and each can measure specific parameters as illustrated in table 1. It is possible to measure all of these parameters using the EBP.

The EBP uses the deflection of low energy electrons due to the fields of the ion beam to provide information about the charge distribution of the ion beam. Using two sets of deflection plates the electron beam is scanned across the ion beam (see Figure 1). With a third set of deflector plates the electron beam is returned to the middle of a position detector. The deflection due to the ion beam is determined by subtracting this third deflector voltage with and without the

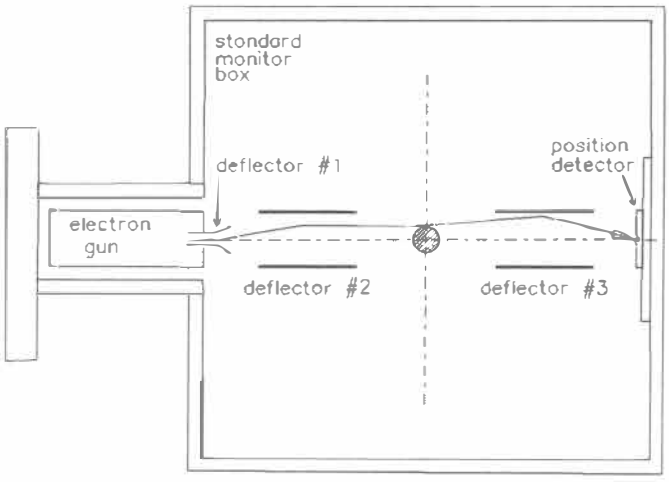

Figure 1: System layout.

ion beam. This difference is then plotted as a function of position to give us a deflection curve. This deflection curve reveals information about the size, centroid, profile, and current of the ion beam. At present we are testing the theory to see the abilities of this system.

2 THEORY

Assume we have an infinitely long cylinder of charge (for DC ion beams) in the z direction circularly symmetric , centred at $x = y = 0$ (see Figure 2). Assume an electron trajectory initially parallel to the x axis moving at constant y from $x = -x_\bullet$ to $x = x_f$. That is, we assume the deflection due to the ion beam is small so that we can approximate $y = y_o$. Let the ion beam radius be a. Let the ion beam charge density ρ be given by

$$\rho = \left[1 - \left(\frac{r}{a}\right)^2\right]^{m-1}$$

where m characterizes the charge distribution. The fraction of beam f inside radius r is

$$f = 1 - \left[1 - \left(\frac{r}{a}\right)^2\right]^m$$

Figure 3 shows the radial charge density and fraction of the beam for various values of m. Note that for $m = 1$ we have a uniform density and then $f = (\frac{r}{a})^2_{r<a}$.
By Gauss' Law the radial electric field component due to the ion beam for $r > a$ is given by

$$E_r = \frac{\lambda}{2\pi\varepsilon_o r}$$

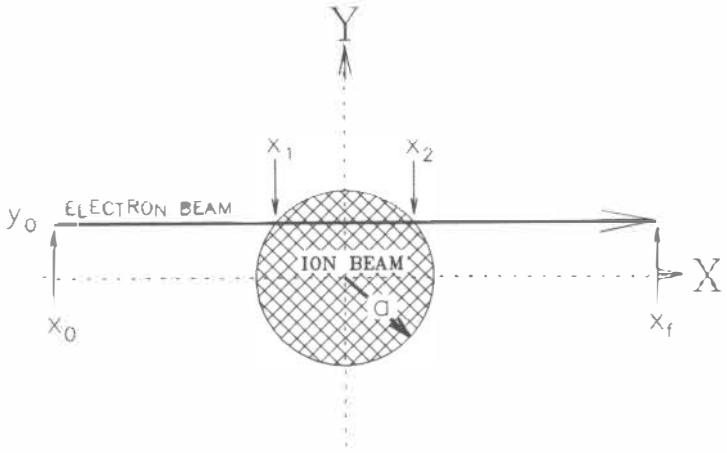

Figure 2: Assumed electron trajectory.

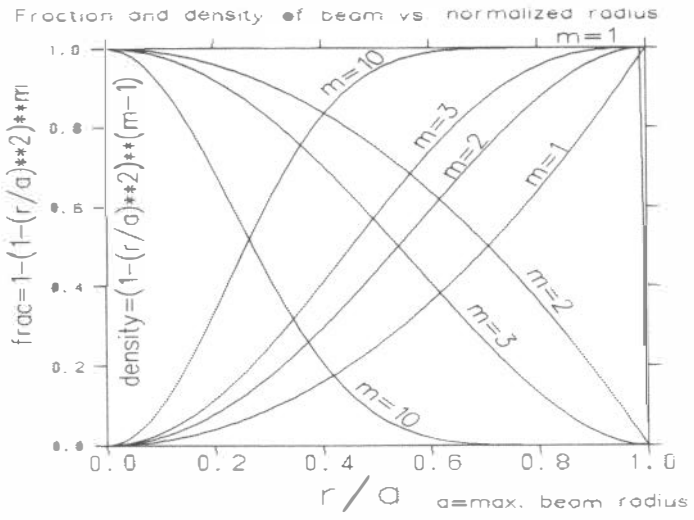

Figure 3: Radial charge density and beam fraction vs. normalized radius for various m

where λ is the linear charge density
and the permittivity of free space $\varepsilon_o = 8.8542 \times 10^{-12}$ coulombs^2/newton·meter^2.
Then the y component of the electric field is

$$E_y = \frac{\lambda}{2\pi\varepsilon_o r}\left(\frac{y}{r}\right) = \frac{\lambda y}{2\pi\varepsilon_o(x^2+y^2)}$$

For $x^2 + y^2 < a$ the linear charge density of a point inside the ion beam radius is given by the total linear charge density multiplied by the fraction of the beam

$$\lambda f = \lambda\left(1 - \left[1 - \left(\frac{r}{a}\right)^2\right]^m\right)$$

The electric field at this point then becomes

$$E_y = \frac{\lambda y}{2\pi\varepsilon_o(x^2+y^2)} - \frac{\lambda\left(1 - \frac{x^2}{a^2} - \frac{y^2}{a^2}\right)^m y}{2\pi\varepsilon_o(x^2+y^2)}$$

which for $m = 1$ simplifies to

$$E_y = \frac{\lambda y}{2\pi\varepsilon_o a^2}$$

The deflection of the electron beam v_y due to the electric field of the ion beam is given by

$$v_y = \int_{t_o}^{t_f} \frac{q_e E_y}{m_e} dt$$

and assuming the x velocity v_x =constant

$$v_y = \int_{x_o}^{x_f} \frac{q_e E_y}{m_e v_x} dx$$

where the charge of the electron $q_e = -1.602189 \times 10^{-19}$ coulombs
and the mass of the electron $m_e = 9.109534 \times 10^{-31}$ kg.

Case $y > r$ (all m)

$$v_y = \frac{q_e \lambda}{2\pi\varepsilon_o m_e v_x}\{atan(x_f/y) - atan(x_o/y)\}$$

Case $y < r$ ($m = 1$)

Figure 2 shows the path over which the electric field is integrated.

$$v_y = \int_{x_o}^{x_1} \frac{q_e}{m_e v_x}\frac{\lambda}{2\pi\varepsilon_o}\frac{y}{(x^2+y^2)}dx + \int_{x_1}^{x_2} \frac{q_e}{m_e v_x}\frac{\lambda y}{2\pi\varepsilon_o a^2}dx + \int_{x_2}^{x_f} \frac{q_e}{m_e v_x}\frac{y}{2\pi\varepsilon_o(x^2+y^2)}dx$$

$$v_y = \frac{q_e\lambda}{2\pi\varepsilon_o m_e v_x}\left\{atan(x_1/y) - atan(x_o/y) + atan(x_f/y) - atan(x_2/y) + 2\sqrt{a^2-y^2}\frac{y}{a^2}\right\}$$

where $x_1 = -\sqrt{a^2-y^2}$ and $x_2 = \sqrt{a^2-y^2}$

Case $y < r$ $(m = 3)$

$$v_y = \frac{q_e\lambda}{2\pi\varepsilon_o m_e v_x}\left\{\int_{x_o}^{x_1}\frac{y}{x^2+y^2}dx + \int_{x_2}^{x_f}\frac{y}{x^2+y^2}dx + \int_{x_1}^{x_2}\frac{y}{x^2+y^2}dx - \int_{x_1}^{x_2}\frac{y\left(1-\frac{x^2}{a^2}-\frac{y^2}{a^2}\right)^3}{x^2+y^2}dx\right\}$$

$$\begin{aligned} v_y &= \frac{q_e\lambda}{2\pi\varepsilon_o m_e v_x}\left\{atan\left(\frac{x}{y}\right)\Big|_{x_o}^{x_1} + atan\left(\frac{x}{y}\right)\Big|_{x_2}^{x_f} + atan\left(\frac{x}{y}\right)\Big|_{x_1}^{x_2} - atan\left(\frac{x}{y}\right)\Big|_{x_1}^{x_2}\right. \\ &\quad \left. + \left\{\frac{3xy}{a^2} - \frac{(3xy^3+x^3y)}{a^4} + \frac{\left(xy^5+\frac{2}{3}x^3y^3+\frac{1}{5}x^5y\right)}{a^6}\right\}\Big|_{x_1}^{x_2}\right. \end{aligned}$$

$$\begin{aligned} v_y &= \frac{q_e\lambda}{2\pi\varepsilon_o m_e v_x}\left\{atan\left(\frac{x_1}{y}\right) - atan\left(\frac{x_o}{y}\right) + atan\left(\frac{x_f}{y}\right) - atan\left(\frac{x_2}{y}\right)\right. \\ &\quad \left. + \frac{6xy}{a^2} - \frac{6xy^3}{a^4} - \frac{2x^3y}{a^4} + \frac{2xy^5}{a^6} + \frac{4x^3y^3}{3a^6} + \frac{2x^5y}{5a^6}\right\} \end{aligned}$$

where $x = x_2 = -x_1$

Analytic solutions for other integral and half integral values of m were calculated using SMP (Symbolic Manipulation Program).

As shown in Figure 1 deflector plate #3 is used to return the electron beam to the middle of the position detector. Using the layout as shown in Figure 4 we can calculate the electric field (and hence the plate voltage) required to do this given the initial vertical velocity v_{y_o} and position y_o

$$y_f = y_1 + \frac{v_{y_1}l_2}{v_x} = 0$$

Also

$$y_1 = y_o + \frac{v_{y_o}l_1}{v_x} + \frac{1}{2}\frac{q_e\mathcal{E}}{m_e}\left(\frac{l_1}{v_x}\right)^2$$

where $\mathcal{E}$ is the electric field between the deflection plates

Also

$$v_{y_1} = v_{y_o} + \frac{q_e\mathcal{E}}{m_e}\frac{l_1}{v_x}$$

Eliminating y_1 and v_{y_1} gives

$$\mathcal{E} = \frac{-m_e\left(y_o + v_{y_o}\left(\frac{l_1}{v_x}+\frac{l_2}{v_x}\right)\right)}{q_e\left(\frac{l_1l_2}{v_x^2}+\frac{l_1l_1}{2v_x^2}\right)}$$

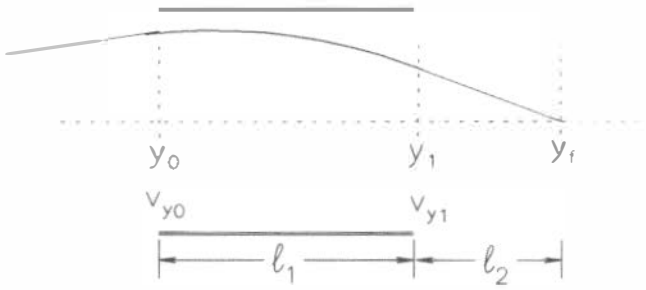

Figure 4: Electron trajectory through deflection plates 3

If we consider parallel scanning the electron beam in the y-direction the difference in the electric field of the third deflector with and without the ion beam is given by

$$\Delta\mathcal{E} = \mathcal{E}_3' - \mathcal{E}_3 = \frac{-m_e\left(y_o' + v_{y_o}\left(\frac{l_1}{v_x} + \frac{l_2}{v_x}\right)\right) + my_o}{q_e\left(\frac{l_1 l_2}{v_x^2} + \frac{l_1 l_1}{2v_x^2}\right)}$$

where $y_o' = y_o + \frac{x_f v_y}{v_x}$ represent the increase in y_o due to the ion beam. This gives

$$\Delta\mathcal{E} = \frac{-2m_e v_x v_{y_o}\{x_f + l_1 + l_2\}}{q_e l_1 \quad 2l_2 + l_1}$$

Which if we substitute in the value for v_{y_o} derived earlier

$$v_{y_o} = \int_{x_o}^{x_f} \frac{q_e E_y}{m_e v_x} dx$$

The equation becomes

$$\Delta\mathcal{E} = \frac{-2\{x_f + l_1 + l_2\}}{l_1 \quad 2l_2 + l_1} \int_{x_o}^{x_f} E_y dx$$

Notice that this difference in deflector plate voltage is solely dependent on the ion beam and the fixed geometry of the system. This difference is independent of the electron charge, mass and energy.

It is this difference which is plotted against position in the y direction which gives us a deflection curve. The deflection curve allows us to extract information about the charge distribution of the ion beam.

3 SYSTEM DESIGN

The system design for the first stage of testing was chosen to give us flexibility in checking the theory. The system design was similar to that shown in Figure 1.

The electron gun chosen was the PHI Model 04-015 Auxiliary Electron Gun produced by Physical Electronics Industries Inc. The gun is equipped with a tungsten filament which can tolerate repeated exposure to atmospheric pressure without adverse effects. According to the manufacture's specifications the electron gun is capable of beam energies up to 5KV, beam currents greater than 100μA, and a focused beam size of less than 0.5mm diameter.

The electron gun also comes equipped with a vertical and horizontal deflector. The horizontal deflector compensated for outside influences, thereby horizontally centering the beam on the position detector. The vertical deflector was used to move the electron beam in the vertical direction. The second deflector consisted of two copper plates 50mm square separated by 20mm (see Figure A1 in appendix). The second deflector was used to make the electron beam parallel to the x axis to allow parallel scanning of the ion beam. We can then scan the ion beam in the y direction by simply changing the initial angle of the electron beam using deflector #1 and changing the voltage of deflector #2 to make the electron beam parallel to the x axis.

The position detector was simply two copper plates 10mm square separated by 0.01mm (see Figure A2 in appendix). Each copper plate was connected to a differential amplifier. When the electron beam is balanced in the middle of the position detector the differential amplifier will give a zero signal which was taken as our zero position in the y direction. The signal quality and sensitivity were the reasons for selecting this method of detecting the zero position. The third deflector, which was similar to the second, was used to return the electron beam, if it were deflected either by scanning voltages and/or the ion beam, to the middle of the position detector to generate this zero signal. To reduce secondary emission the position detector was biased to +90V.

Because we used low energy electrons (1-2 KeV) we were very sensitive to stray magnetic fields. To protect against external stray magnetic fields from the cyclotron (approximately 10G in our location) and from focusing solenoids nearby, we used a soft iron pipe around the electron gun and a sheet of mu-metal inside the vacuum chamber. The mu-metal was wrapped around the electron beam's path with a hole in the side to allow the ion beam to pass through (see Figure A3 in appendix). This reduced the effects of the external magnetic fields to the point where we could operate the device.

The vacuum system required a pressure of less than 10^{-8} Torr to operate the electron gun. This pressure was reached with a combination of turbopumps and cryopumps. In addition to this we also required the ability to quickly vent the system (in less than 15 minutes) to allow us to modify our system with ease. Our system required 7 high vacuum feedthroughs as well as an additional 5 feedthroughs located on the electron gun.

4 COMPUTER SIMULATION

The original computer simulations were carried out with a ray tracing program called TRIWHEEL. Using TRIWHEEL Figure 5 was produced for a 600μA ion beam at 25KeV and having a radius of 5mm. U_3 is the third deflector voltage necessary to return the electron beam to the middle of the position detector with no ion beam deflection and U_3' is the voltage of the

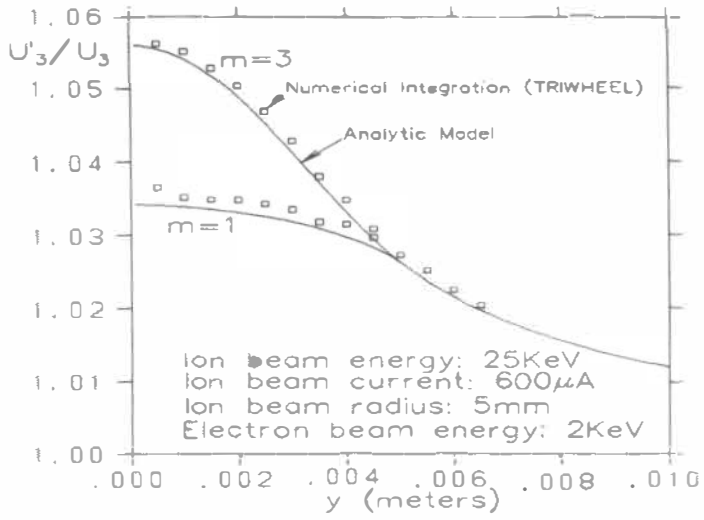

Figure 5: Comparison of the ray tracing code TRIWHEEL with the analytic model.

third deflector with the added deflection due to the ion beam. From Figure 5 we see that the change is about 5.5% for the gaussian m=3 distribution while it is only about 3.5% for the m=1 or uniform ion distribution. We then developed an approximate analytic solution which was considerably faster than using TRIWHEEL. The analytic solution agreed well with the raytracing code TRIWHEEL as shown in Figure 5.

We checked the sensitivity of our system for different parameters of the EBP using the analytic model. Figure 6 shows the maximum deflection of the electron beam vs. the electron beam energy as calculated analytically for a 500μA 15KeV ion beam. While Figure 7 shows the deflection vs. ion beam current for various electron beam energies. This gives us a measure of the sensitivity of the EBP for various electron beam energies. Note that for our integration from $-\infty$ to $+\infty$ the deflection is independent of y providing y exceeds the ion beam radius a. From these results we chose the energy of the EBP to be between 1 and 2 KeV to measure ion beam currents in the range of greater than 200μA with ion beam energies of between 15 and 300 KeV.

It was found that subtracting U_3'-U_3 was more useful than the ratio of voltages. A typical deflection curve (U_3'-U_3 vs y) is shown in Figure 8. Figure 8 was produced, using the analytic model, for an ion beam centred at x=y=0, an energy of 15KeV, a current of 500μA, and a uniform density (m=1). Figure 9 shows deflection curves for various ion beam density distributions (various m values). There is a symmetric portion of the deflection curve for negative y values which is not shown in Figure 9.

The derivative of the deflection curve (U_3'-U_3 vs Y) with respect to Y is related to the projection onto the Y axis of the X-Y ion beam distribution. As seen in Figure 10 the derivative of the deflection curve is in good agreement with this ion beam projection. The agreement gets better as the density of the ion beam increases. The derivative of the deflection curve was normalized to make direct comparisons to the density function easier.

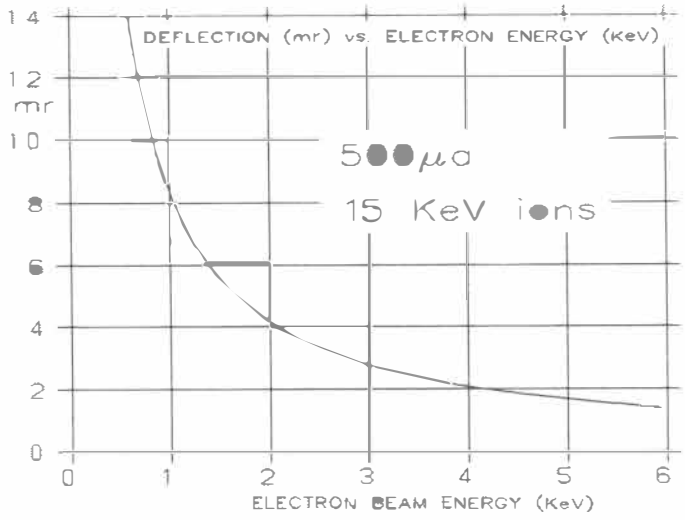

Figure 6: Maximum electron beam deflection vs. electron energy.

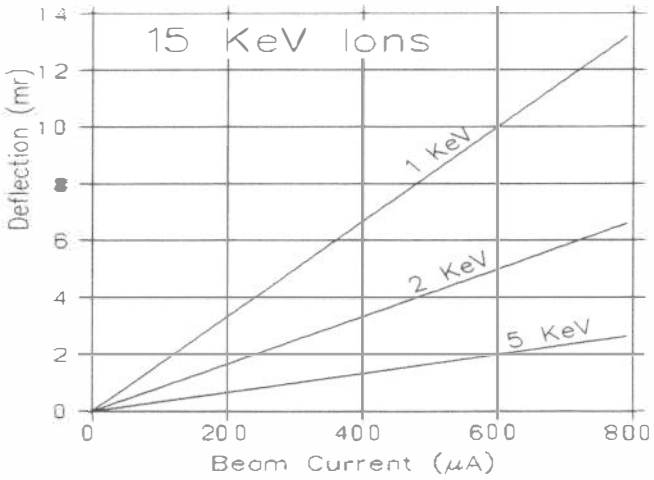

Figure 7: Electron beam deflection vs. ion beam current for various electron beam energies.

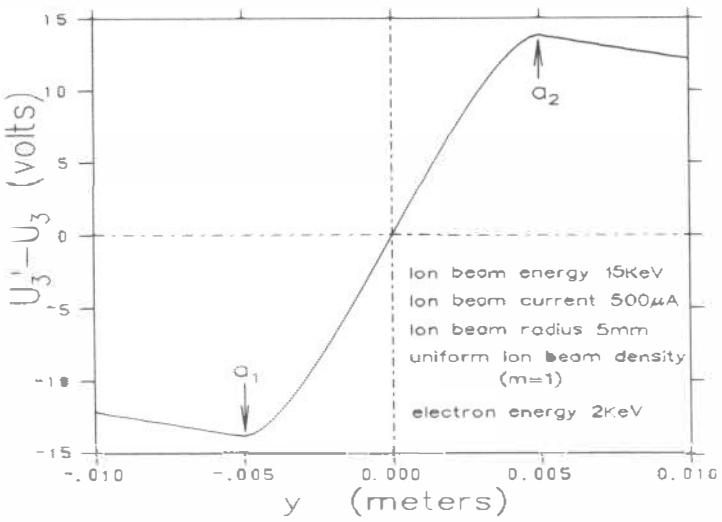

Figure 8: Deflection curve resulting from a uniform ion beam density.

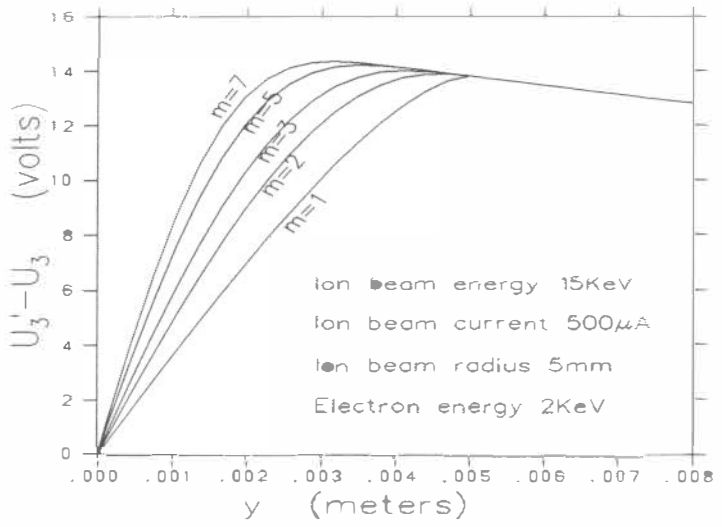

Figure 9: Deflection curves for various ion beam density distributions.

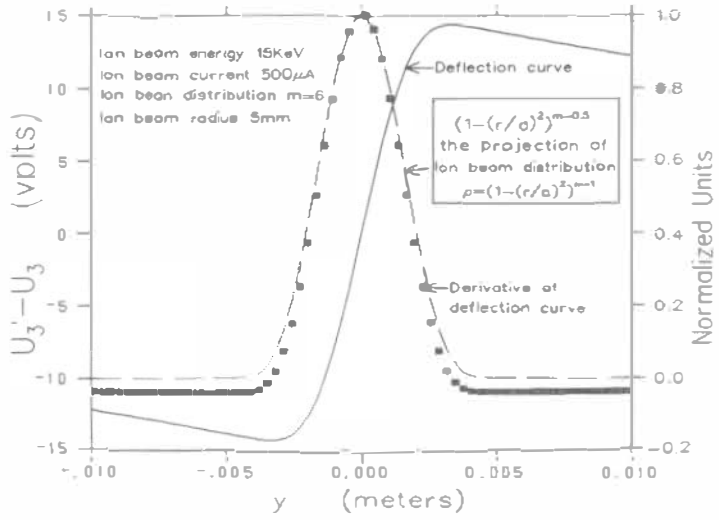

Figure 10: Projection of ion beam distribution compared to derivative of the deflection curve.

Using the computer simulations it was found that we could measure:

1. The size of the ion beam by the separation of the points of maximum deflection (eg. points a_1 and a_2 in Figure 8).
2. The position of the center of the ion beam – ie. the position of no deflection.
3. The symmetry of the beam from the symmetry of the deflection curve.
4. The profile of the beam from the shape of the deflection curve.
5. The beam current from the magnitude of the peak deflection.
6. The neutralization by comparing the deflection curve of a neutralized and an unneutralized beam.

Figure 11 shown simulations for 3 different beam distributions. Note again how well the normalized derivatives of the deflection curves agree with the projected beam density.
The following is a listing of the OPDATA macro used to calculate the deflection curve for any "beamlet". By adding two (or more) such beamlets together we can calculate the deflection curves due to more complex ion beam distributions (as in Figures 11). The projected beam densities are readily calculated by summing the binomial distributions with m replaced by m+0.5. See reference 10 for details.

```
XM= ?       !  FIRST MACRO PARAMETER IS THE 'M' OF THE ION BEAM
XC= ?       !  X CENTRE SHIFT OF ION BEAM (METERS)
YC= ?       !  Y CENTER SHIFT OF ION BEAM  (METERS)
R= ?        !  RADIUS OF ION BEAM IN METERS
Q= ?        !  CHARGE/METER OF ION BEAM=PARAM(15)/PARAM(58)
```

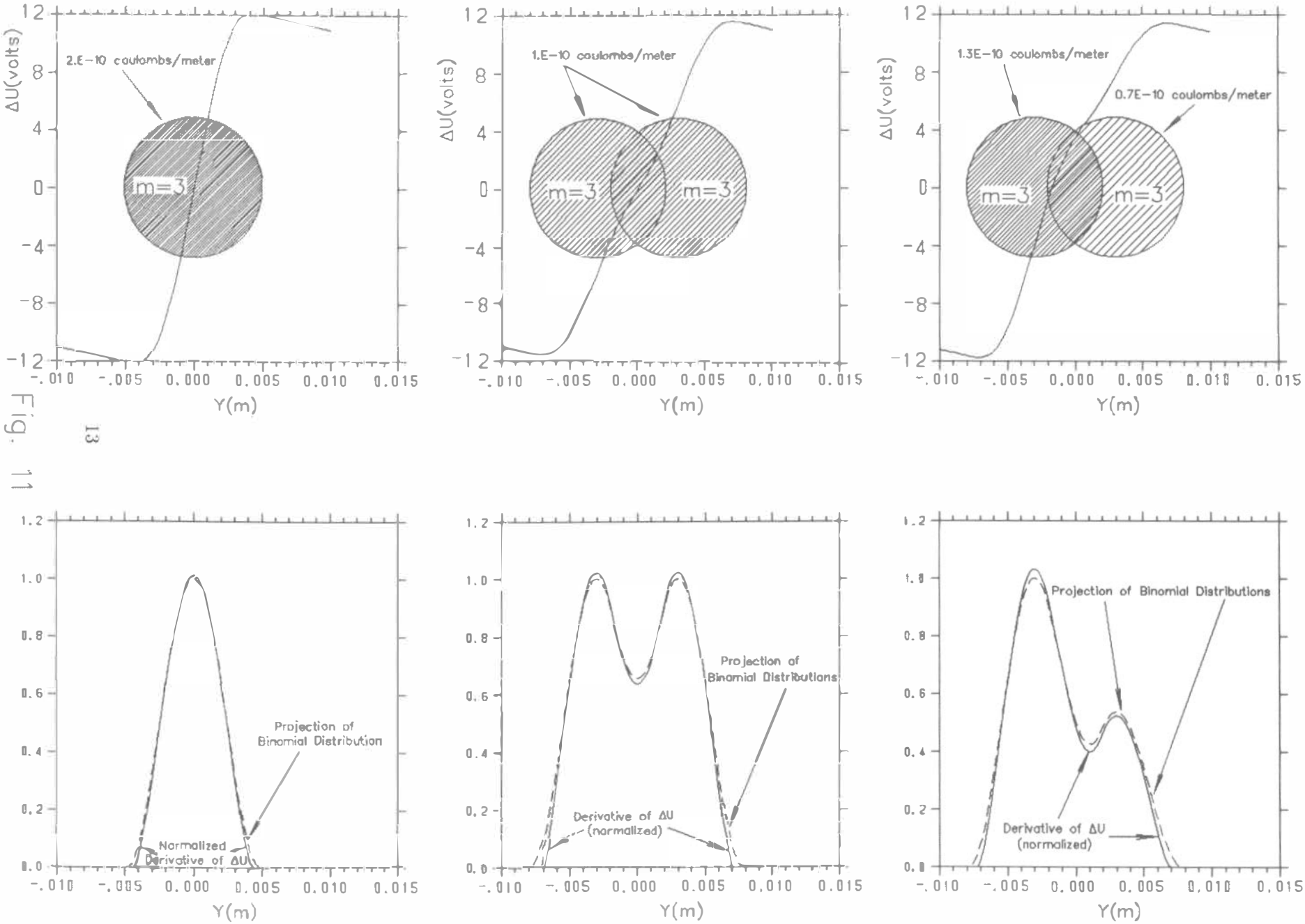
ΔU(volts)
Y(m)
2.E-10 coulombs/meter
m=3
1.E-10 coulombs/meter
m=3
m=3
1.3E-10 coulombs/meter
0.7E-10 coulombs/meter
m=3
m=3
Projection of Binomial Distribution
Normalized Derivative of ΔU
Projection of Binomial Distributions
Derivative of ΔU (normalized)
Projection of Binomial Distributions
Derivative of ΔU (normalized)

Fig. 11

```
L1=0.042   !  DEFLECTOR LENGTH IN METERS
L2=0.020   !  DISTANCE FROM DEFLECTOR EXIT TO FOCUS
XO=-0.038+XC  !  STARTING X VALUE OF ELECTRON BEAM
XF=0.038-XC   !  STARTING X VALUE OF DEFLECTOR
QE=1.6020E-19          ! ELECTRON CHARGE IN COULOMBS
EO=8.854E-12           ! PERMITTIVITY
M=9.1095E-31           ! ELECTRON MASS IN KG.
VX=2.63E7              ! ELECTRON VELOCITY IN METERS/SEC
PI=3.1415926
C1=QE*Q/2/PI/EO/M/VX   ! CONSTANT FOR VY
RMAX=0.010             ! +/- Y RANGE OF CALCULATION
Y=-RMAX+2*RMAX*(I-1)/99.+RMAX/100000. ! ARRAY OF Y VALUE TO CALCULATE DV
/VECTOR Y 100          ! SET LENGTH TO 100 ELEMENTS
X1=-SQRT(ABS(R**2-(Y-YC)**2))*(ABS(Y-YC)<R)   ! FIRST INTERCEPT WITH ION BEAM
X2=+SQRT(ABS(R**2-(Y-YC)**2))*(ABS(Y-YC)<R)   ! SECOND INTERCEPT WITH ION BEAM
X=+SQRT(ABS(R**2-(Y-YC)**2))*(ABS(Y-YC)<R)     ! X INTERCEPT WITH ION BEAM
T1=ATAN(X1/(Y-YC))                    ! FIRST TERM FOR VY
T2=-ATAN(XO/(Y-YC))                   ! SECOND TERM FOR VY
T3=ATAN(XF/(Y-YC))                    ! THIRD TERM FOR VY
T4=-ATAN(X2/(Y-YC))                   ! FOURTH TERM FOR VY
T5=USERN(XM,X,Y-YC,R)                ! FIFTH TERM FOR VY
VY=C1*(T1+T2+T3+T4+T5) !VELOCITY IN Y OF ELECTRON BEAM AT DEFL. ENTRANCE
DV=2*M/QE*VX*VY/L1*(XF+L1+L2)/(2*L2+L1) ! VOLTAGE DIFF: BEAM ON-BEAM OFF
/PL (Y,DV)
```

where

```
      DOUBLE PRECISION FUNCTION T5(XM,X,Y,R)
C=======================================================================
C==  OPDATA callable function to return T5 term for electron beam
C==  deflection simulation.
C=======================================================================
      IMPLICIT REAL*8 (A-H,O-Z)
      M=XM
      IF (M.EQ.0) GOTO 100
      IF (M.EQ.1) GOTO 101
      IF (M.EQ.2) GOTO 102
      IF (M.EQ.3) GOTO 103
      IF (M.EQ.4) GOTO 104
      IF (M.EQ.5) GOTO 105
      IF (M.EQ.6) GOTO 106
      IF (M.EQ.7) GOTO 107
      IF (M.EQ.8) GOTO 108
      IF (M.EQ.9) GOTO 109
      IF (M.EQ.10) GOTO 110
100      T5=0
         GO TO 999
101      T5=-X*Y/R**2
         GO TO 999
102      T5=-2*X*Y/R**2+(X*Y**3+X**3*Y/3)/R**4
         GO TO 999
103      T5=-3*X*Y/R**2+(3*X*Y**3+X**3*Y)/R**4+
     # (-X*Y**5-2*X**3*Y**3/3-X**5*Y/5)/R**6
         GO TO 999
104      T5=-4*X*Y/R**2+(6*X*Y**3+2*X**3*Y)/R**4+
     # (-4*X*Y**5-8*X**3*Y**3/3-4*X**5*Y/5)/R**6+
     # (X*Y**7+X**3*Y**5+3*X**5*Y**3/5+X**7*Y/7)/R**8
         GO TO 999
105      T5=-5*X*Y/R**2+(10*X*Y**3+10*X**3*Y/3)/R**4+
```

```
     # (-10*X*Y**5-20*X**3*Y**3/3-2*X**5*Y)/R**6+
     # (5*X*Y**7+5*X**3*Y**5+3*X**5*Y**3+5*X**7*Y/7)/R**8+
     # (-X*Y**9-4*X**3*Y**7/3-6*X**5*Y**5/5-4*X**7*Y**3/7-X**9*Y/9)/
     # R**10
         GO TO 999
106      T5=-6*X*Y/R**2+(15*X*Y**3+5*X**3*Y)/R**4+
     # (-20*X*Y**5-40*X**3*Y**3/3-4*X**5*Y)/R**6+
     # (15*X*Y**7+15*X**3*Y**5+9*X**5*Y**3+15*X**7*Y/7)/R**8+
     # (-6*X*Y**9-8*X**3*Y**7-36*X**5*Y**5/5-24*X**7*Y**3/7-2*X**9*Y/3)
     # /R**10+(X*Y**11+5*X**3*Y**9/3+2*X**5*Y**7+10*X**7*Y**5/7+
     # 5*X**9*Y**3/9+X**11*Y/11)/R**12
         GO TO 999
107      T5=-7*X*Y/R**2+(21*X*Y**3+7*X**3*Y)/R**4+
     # (-35*X*Y**5-70*X**3*Y**3/3-7*X**5*Y)/R**6+
     # (35*X*Y**7+35*X**3*Y**5+21*X**5*Y**3+5*X**7*Y)/R**8+
     # (-21*X*Y**9-28*X**3*Y**7-126*X**5*Y**5/5-12*X**7*Y**3-
     # 7*X**9*Y/3)/R**10+(7*X*Y**11+35*X**3*Y**9/3+14*X**5*Y**7+
     # 10*X**7*Y**5+35*X**9*Y**3/9+7*X**11*Y/11)/R**12+
     # (-X*Y**13-2*X**3*Y**11-3*X**5*Y**9-20*X**7*Y**7/7-
     # 5*X**9*Y**5/3-6*X**11*Y**3/11-X**13*Y/13)/R**14
         GO TO 999
108      T5=-8*X*Y/R**2+(28*X*Y**3+28*X**3*Y/3)/R**4+
     # (-56*X*Y**5-112*X**3*Y**3/3-56*X**5*Y/5)/R**6+
     # (70*X*Y**7+70*X**3*Y**5+42*X**5*Y**3+10*X**7*Y)/R**8+
     # (-56*X*Y**9-224*X**3*Y**7/3-336*X**5*Y**5/5-32*X**7*Y**3-
     # 56*X**9*Y/9)/R**10+(28*X*Y**11+140*X**3*Y**9/3+56*X**5*Y**7+
     # 40*X**7*Y**5+140*X**9*Y**3/9+28*X**11*Y/11)/R**12+
     # (-8*X*Y**13-16*X**3*Y**11-24*X**5*Y**9-160*X**7*Y**7/7-
     # 40*X**9*Y**5/3-48*X**11*Y**3/11-8*X**13*Y/13)/R**14+
     # (X*Y**15+7*X**3*Y**13/3+21*X**5*Y**11/5+5*X**7*Y**9+
     # 35*X**9*Y**7/9+21*X**11*Y**5/11+7*X**13*Y**3/13+X**15*Y/15)/R**16
         GO TO 999
109      T5=-9*X*Y/R**2+(36*X*Y**3+12*X**3*Y)/R**4+
     # (-84*X*Y**5-56*X**3*Y**3-84*X**5*Y/5)/R**6+
     # (126*X*Y**7+126*X**3*Y**5+378*X**5*Y**3/5+18*X**7*Y)/R**8+
     # (-126*X*Y**9-168*X**3*Y**7-756*X**5*Y**5/5-72*X**7*Y**3-
     # 14*X**9*Y)/R**10+(84*X*Y**11+140*X**3*Y**9+168*X**5*Y**7+
     # 120*X**7*Y**5+140*X**9*Y**3/3+84*X**11*Y/11)/R**12+
     # (-36*X*Y**13-72*X**3*Y**11-108*X**5*Y**9-720*X**7*Y**7/7-
     # 60*X**9*Y**5-216*X**11*Y**3/11-36*X**13*Y/13)/R**14+
     # (9*X*Y**15+21*X**3*Y**13+189*X**5*Y**11/5+45*X**7*Y**9+
     # 35*X**9*Y**7+189*X**11*Y**5/11+63*X**13*Y**3/13+
     # 3*X**15*Y/5)/R**16+(-X*Y**17-8*X**3*Y**15/3-28*X**5*Y**13/5
     # -8*X**7*Y**11-70*X**9*Y**9/9-56*X**11*Y**7/11-
     # 28*X**13*Y**5/13-8*X**15*Y**3/15-X**17*Y/17)/R**18
         GO TO 999
110      T5=-10*X*Y/R**2+(45*X*Y**3+15*X**3*Y)/R**4+
     # (-120*X*Y**5-80*X**3*Y**3-24*X**5*Y)/R**6+
     # (210*X*Y**7+210*X**3*Y**5+126*X**5*Y**3+30*X**7*Y)/R**8+
     # (-252*X*Y**9-336*X**3*Y**7-1512*X**5*Y**5/5-144*X**7*Y**3
     # -28*X**9*Y)/R**10+(210*X*Y**11+350*X**3*Y**9+420*X**5*Y**7
     # +300*X**7*Y**5+350*X**9*Y**3/3+210*X**11*Y/11)/R**12+
     # (-120*X*Y**13-240*X**3*Y**11-360*X**5*Y**9-2400*X**7*Y**7/7
     # -200*X**9*Y**5-720*X**11*Y**3/11-120*X**13*Y/13)/R**14+
     # (45*X*Y**15+105*X**3*Y**13+189*X**5*Y**11+225*X**7*Y**9+
     # 175*X**9*Y**7+945*X**11*Y**5/11+315*X**13*Y**3/13+
     # 3*X**15*Y)/R**16+(-10*X*Y**17-80*X**3*Y**15/3-56*X**5*Y**13-
     # 80*X**7*Y**11-700*X**9*Y**9/9-560*X**11*Y**7/11-
     # 280*X**13*Y**5/13-16*X**15*Y**3/3-10*X**17*Y/17)/R**18+
     # (X*Y**19+3*X**3*Y**17+36*X**5*Y**15/5+12*X**7*Y**13+
     # 14*X**9*Y**11+126*X**11*Y**9/11+84*X**13*Y**7/13+
```

```
     # 12*X**15*Y**5/5+9*X**17*Y**3/17+X**19*Y/19)/R**20
999   T5=-T5*2.
      RETURN
      END
```

5 SYSTEM ELECTRONICS

Several pieces of prototype electronics were built as part of the development system. The block diagram is shown in Figure A11 of the appendix.

A Bertran HV power supply was used to bias the filament of the electron gun between –1KV and –2KV. The DC filament supply was built using a fullwave bridge rectifier and a 6.3V, 4A transformer with 2500 volts isolation. The filament current was controlled by a 120V variable transformer in the primary circuit. The focusing potentials (535V for 2KeV electrons and 280V for 1KeV) were derived from the second channel of the Bertran HV power supply.

A total of three pairs of deflection plates are used in the system. Each pair is driven in push-pull mode so that the deflection of the electron beam is linear and symmetrical with respect to the center line of the system. Six deflection amplifiers (see Figure A4 of appendix) were built to provide output swings of up to ±170V for control signals of less than ±5V. It was found that the control of the beam did not require deflection voltages greater than ±80V for the first deflector and the gain of its deflection amplifier was later reduced. The bandwidth of the deflection amplifiers are greater than 10 KHz which is more than adequate for programmed scanning of the electron beam in the range ±7mm. The deflection power supply was built using a 240V center tapped transformer which limits the maximum deflection voltage to ±170V. The first and second pairs of deflection plates are used to displace the electron beam vertically and steer it parallel to the centre line. The deflection voltage on these two deflection plates were manually controlled in the initial development with an accuracy of approximately 0.1V. The voltage on deflector plates #2, to generate a parallel beam, is determined by geometrically scaling the voltage on this plate required to give a centred beam on the position detector *without an ion beam.* A third pair of deflection plates were used to sweep the beam back across the detector plates. The 1Hz sawtooth drive signal for the 3rd deflection plates was provided by a commercial signal generator (see the typical shape of the drive signal and the position detector signal in Figure A5 of appendix). The amplitude of the sawtooth drive signal was ±5V peak to peak.

The system uses a null detector to sense the 3rd deflection plate voltage necessary to return the electron beam to the center of the two detector plates. Each position detector plate is connected to an input of the differential current amplifier (see Figure A6 of appendix for schematic of the differential current amplifier). Note the +90V bias used to reduce secondary emission from the detector plates. This bias voltage was necessary to get reliable and reproducible current readings. The bandwidth of the amplifier was limited to 10 Hz to reduce the system sensitivity to 60 Hz interference. When the signal from the differential detector passes through a null, a sample and hold circuit (see Figure A7 of appendix) is triggered to measure the instantaneous sweep voltage at the generator. This value is recorded by an ADC and the result is averaged

and then displayed on an IBM PC.

6 EXPERIMENTAL RESULTS

Before any measurements of the ion beam were taken the system was thoroughly tested. Using a phosphorous screen we adjusted the focusing voltage and optimised the electron gun parameters for energies between 1 and 2KeV. The optimum beam size was approximately 2mm for all energies tested. This was different from the manufactures specifications possibly due to long focusing (the distance in our system from electron gun to phosphorous screen was 200mm).
To achieve parallel scanning of our EBP we built a special position detector (see Figure A8 of appendix) which consisted of 10 separated conducting strips at known positions. We were able to connect any combination of strips to the differential amplifier and read the difference in current on the strips. By zeroing the amplifier signal between neighboring strips we found the position of the electron beam and found the deflector voltage settings for parallel scanning to within ±5degrees. It was found that for parallel scanning the deflector #1 voltage (U_1) was 10V/mm while deflector #2 voltage (U_2) and deflector #3 without ion beam (U_3) was 22V/mm.
To avoid collecting space charge around the deflectors and to make the measurements automatic a sweep generator was connected to the third deflector. This caused the electron beam to be swept over the position detector. Our electronics limited the frequency at which we could operate the sweep generator to 1Hz.
To simulate the ion beam we placed a single copper wire with voltages ranging between 0 and -20 V in the path of the electron beam. These voltages corresponded to the potential of the ion beam we measured. The ratio of U_3'-U_3/V_{wire} was found to be approximately 0.5 for 1KeV electrons and we got deflections that gave reasonable agreement with Figure 7.
In the original design of the third deflector the deflector plates were supported on copper arms. This created some fields between the copper arm and the position detector. As a result the output signal was very noisy because of low energy ions. To eliminate these fields the copper arms were replaced by non conducting supports.
The experimental measurements of the ion beam were made using TRIUMF's I3 ion source of unpolarized H^-.
To define the size of the ion beam we placed a copper plate with a 4.8mm diameter aperture 50mm upstream from the geometric centre of our system (see Figure A9 of appendix). Later this aperture was further reduced to 2mm diameter.
Because the position detector plates were biased to +90V to reduce secondary emission a noise problem was created due to stray ions from the ion source which were attracted to the position detector. To reduce this problem two grounded meshes were placed in front of the position detector which reduced the signal from these stray ions significantly.
Although the magnetic shielding help to reduce the effect of external stray magnetic fields these effects were not eliminated. The stray fields reduced the scanning range of our EBP. We could only move the beam up 4mm and down 7mm. The stray magnetic fields also caused us to doubt how parallel the electron beam's path was. In aligning our system with the centre of the beam pipe we felt the geometric centre of our EBP was within ±1.0mm of the centre of the

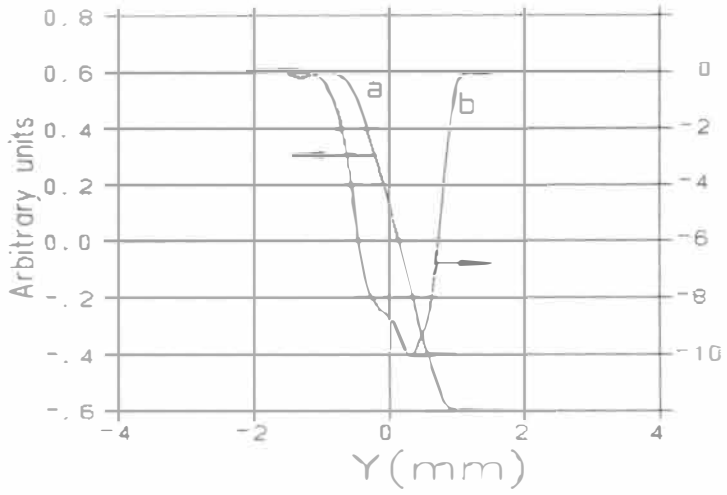

Figure 12: Experimental deflection curve and its derivative.

beam pipe. Approximately 50mm downstream from the centre of our EBP was a wire scanner for measuring beam profiles. We could see the change in beam profile as recorded on the wire scanner when we adjusted the focusing solenoid which was located 500mm upstream from our EBP. This solenoid gave us some control over the ion beam.
Several graphs were produced of U_3'-U_3 vs Y. These graphs gave good agreement with those predicted from the computer simulation. For the experimental results the H^- beam was accelerated to an energy of 15KeV. The beam current was varied between 120μA and 460μA. Figure A10 of appendix shows the experimental deflection curves and ion beam profiles (wire scanner). Figure 12 illustrates the initial attempt to reconstruct the beam profile from the deflection curve. Digitized raw data was interpolated to get a smooth deflection curve (a). The derivative was then taken to reconstruct the beam profile (b). Comparison with the wire scan profile (Figure A10-a of appendix) taken 50mm downstream shows a reasonable agreement. Further work is required to properly cross-calibrate the two techniques. It is essential that future developments gather a continuous deflection curve rather than a few sample points.

7 FUTURE DEVELOPMENTS

There are several improvements that can be made to increase the usefulness of the EBP as a real measuring device.
One of these developments is to increase the speed of the electronics. The initial studies were done with the relatively slow 1 Hz sweep speed because the differential current amplifier was limited to a 10 Hz bandwidth. With better shielding, 60 Hz pickup may become less of a problem and faster sweep speeds could be used. With sweep speeds greater than 1 KHz, one could AC couple the detector amplifier and reject all frequencies below 100 Hz. The output of

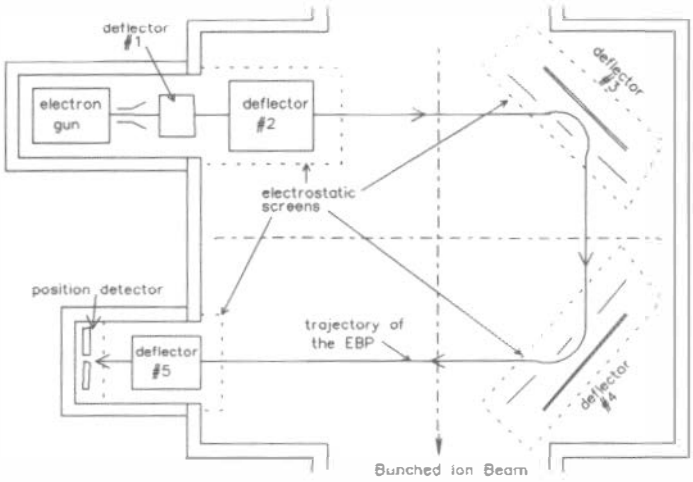

Figure 13: Proposed system for ion beam energy measurement.

the sample and hold detection system could then be low pass filtered to recover the value of the deflection voltage necessary to return the electron beam to the detector center.

The voltages on the first two deflection plates were manually controlled during the development work. These voltages and the voltage on the third deflector can be computer controlled in such a way as to automate the entire measuring process. The computer would first adjust the voltage on the first and second pairs of deflection plates to displace the electron beam vertically and then adjust the third deflector voltage to return the electron beam to the centre of the detector. With repeated measurements at different vertical displacements, the computer could determine the profile of the ion beam.

Another improvement would be to increase the separation of the deflector plates. The current separation is ± 10mm. With increased separation we would be able to measure larger beams.

To reduce the error bars associated with our measurements the EBP should have better stability. The deflector voltages, the high voltage to the electron gun, and the filament current of the electron gun should all be stabilized to 0.05%. Another development that would increase the stability of the EBP would be improved magnetic shielding. Making the entire vacuum box out of soft iron would reduce the effect of stray magnetic fields.

To screen outside electrostatic influences we plan to surround the deflectors with a grounded mesh.

In order to measure any time structure of the beam a more sophisticated system will have to be built as shown in Figure 13. The system would operate with a bunched ion beam. The electron beam would be deflected by the head of the ion beam bunch by some angle according to the relative position of the head of the bunch and the electron beam. This electron beam deflection would be parallel to the ion beam. When the electron beam intersects the ion beam again it will be once more deflected by the head of the ion beam but in the opposite direction.

The position detector would sense the loss of the electron beam if these two deflections are not equal qnd opposite. We can therefore get a measure of the average energy of the ion beam by carefully measuring the electron beam energy corresponding to the case where these two deflections are equal. It would also be possible to get a longitudinal profile of the beam.

8 CONCLUSION

Preliminary results are very promising. They show the the very high sensitivity of the method (we can see deflections of about 5mrad) and the way to construct a real measurement system. The advantage of such a system are clear

- no radiation damage
- no mechanical moving parts
- high level of flexibility
- measure beams of either polarity
- measure beams of current greater than $100\mu A$

9 ACKNOWLEDGEMENTS

We would like to thank the following people for there help and encouragement with Electron Beam Probe: G. Dutto, P. Schmor, M. McDonald, N. England, and W. Fraszer

10 REFERENCES

1. K.B. Unser, "Beam Transformer With DC to 200 Mhz Range", IEEE Trans., NS-16, pp. 934-938, June 1969,

2. C.D. Johnson and L. Thorndall, "The CPS Gas Ionization Beam Scanner", IEEE Trans., Ns-16, 909 (1960).

3. J.C. Denard et al., "Monitoring the Beam Position in the SLC Interaction Region", SLAC-PUB-4267, March 1987.

4. F.B. Kroes et al., "Non-Intercepting High Resolution Beam Monitors", IEEE Trans., NS-28, No.3, pp. 2362-2364, June 1981.

5. A. Hofmann, "Electron and Proton Beam Diagnostics with Synchrotron Radiation", IEEE Trans., NS-28, No.3, pp. 2132-2136, June 1981.

6. W.B. Cottingame et al., "Noninterceptive Techniques for Measurement of Longitudinal Parameters for Intense H^- Beams", IEEE Trans., NS-32, No.5, pp. 1871-1873, (1985).

7. J.S. Fraser, "Developments in Non-Destructive Beam Diagnostics", IEEE Trans, NS-28, No.3, pp. 2137-2141, June 1981.

8. Joseph D. Sherman et al., "Beam Potential Measurement of an Intense H^- Beam by Use of the Emissive Probe Technique", IEEE Trans., NS-32, No.5, pp. 1973-1975, (1985).

9. J. Shiloh, M. Lampel, and R. Sah, "Electron Beam Probe For Charge Neutralization Studies of Heavy Ion Beams", LBL-14391, June 1982.

10. W. Joho, "Representation of Beam Ellipses for Transport Calculations", SIN-Report TM-11-14 (1980).

11 APPENDIX

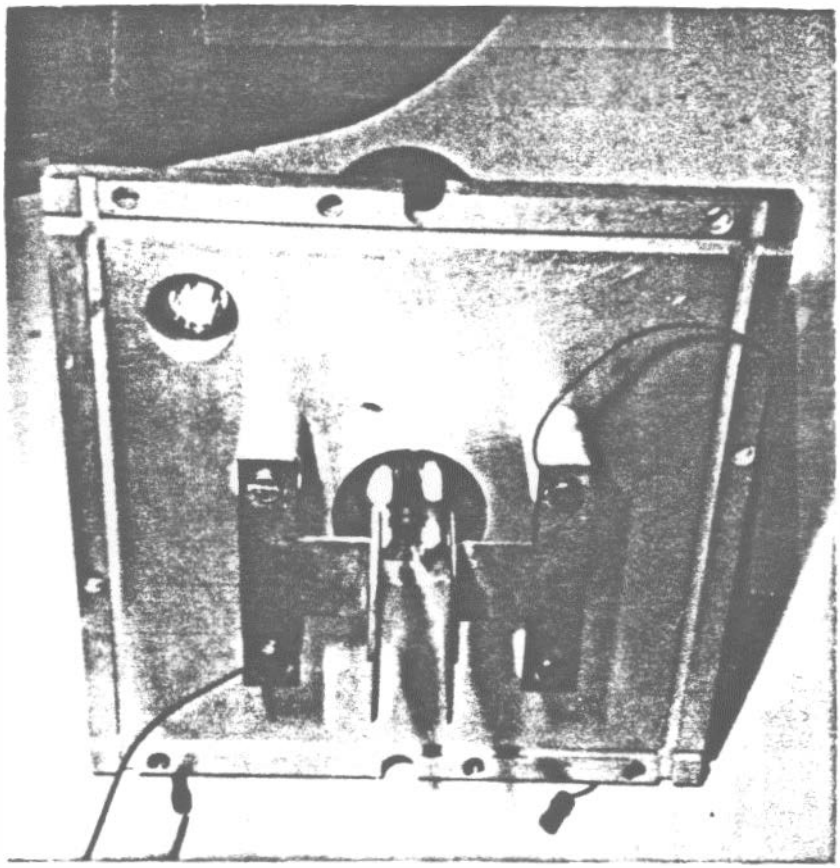

Fig. 1

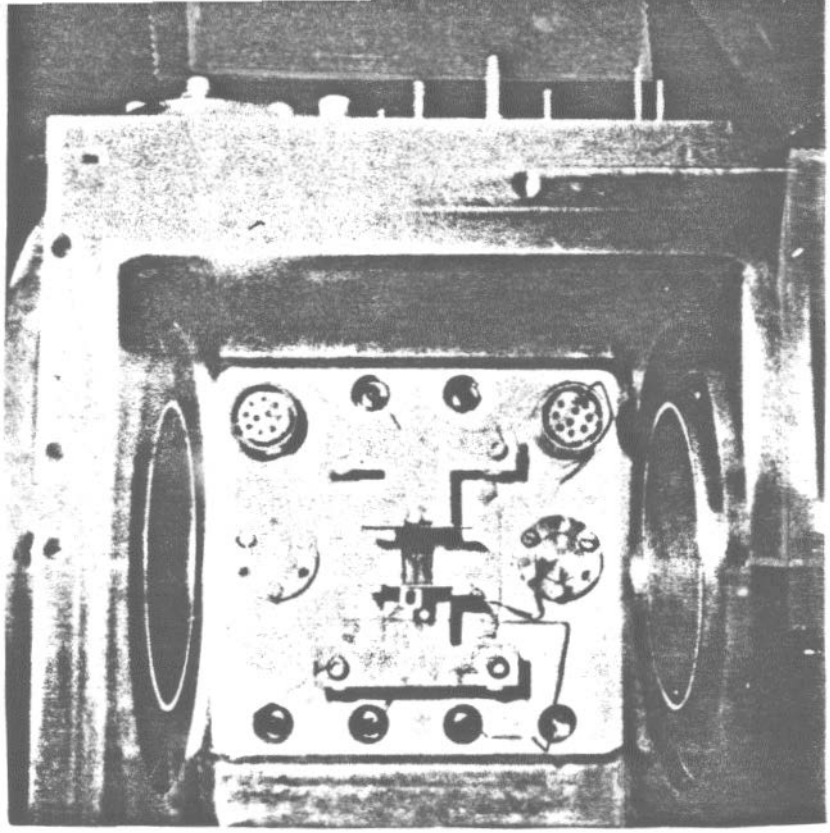

Fig. 2

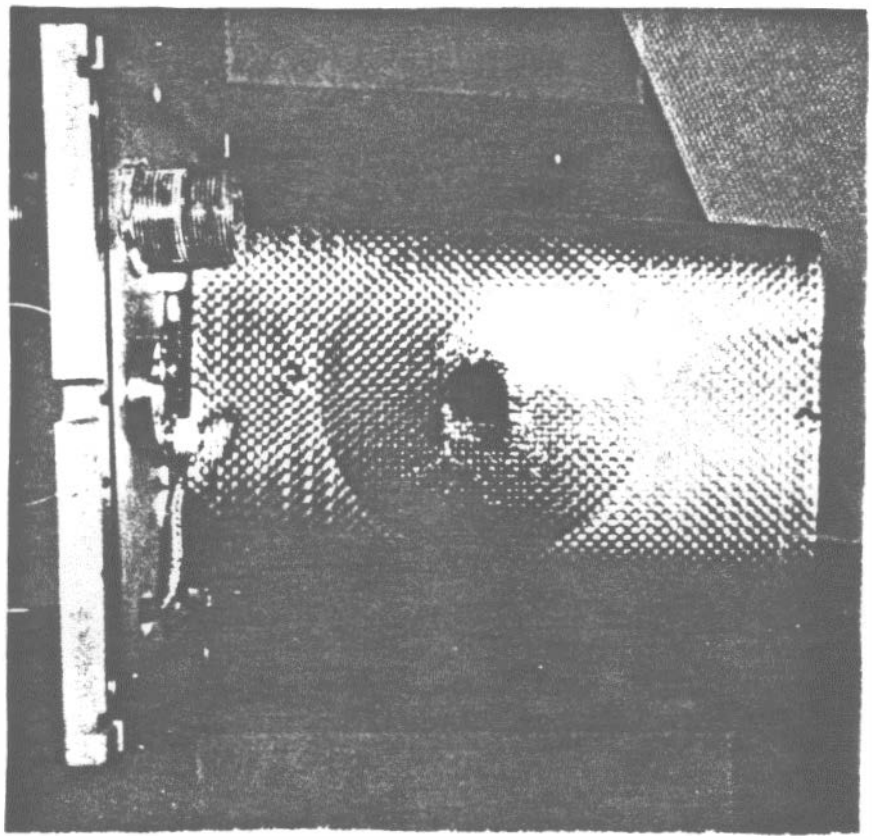

Fig. 3

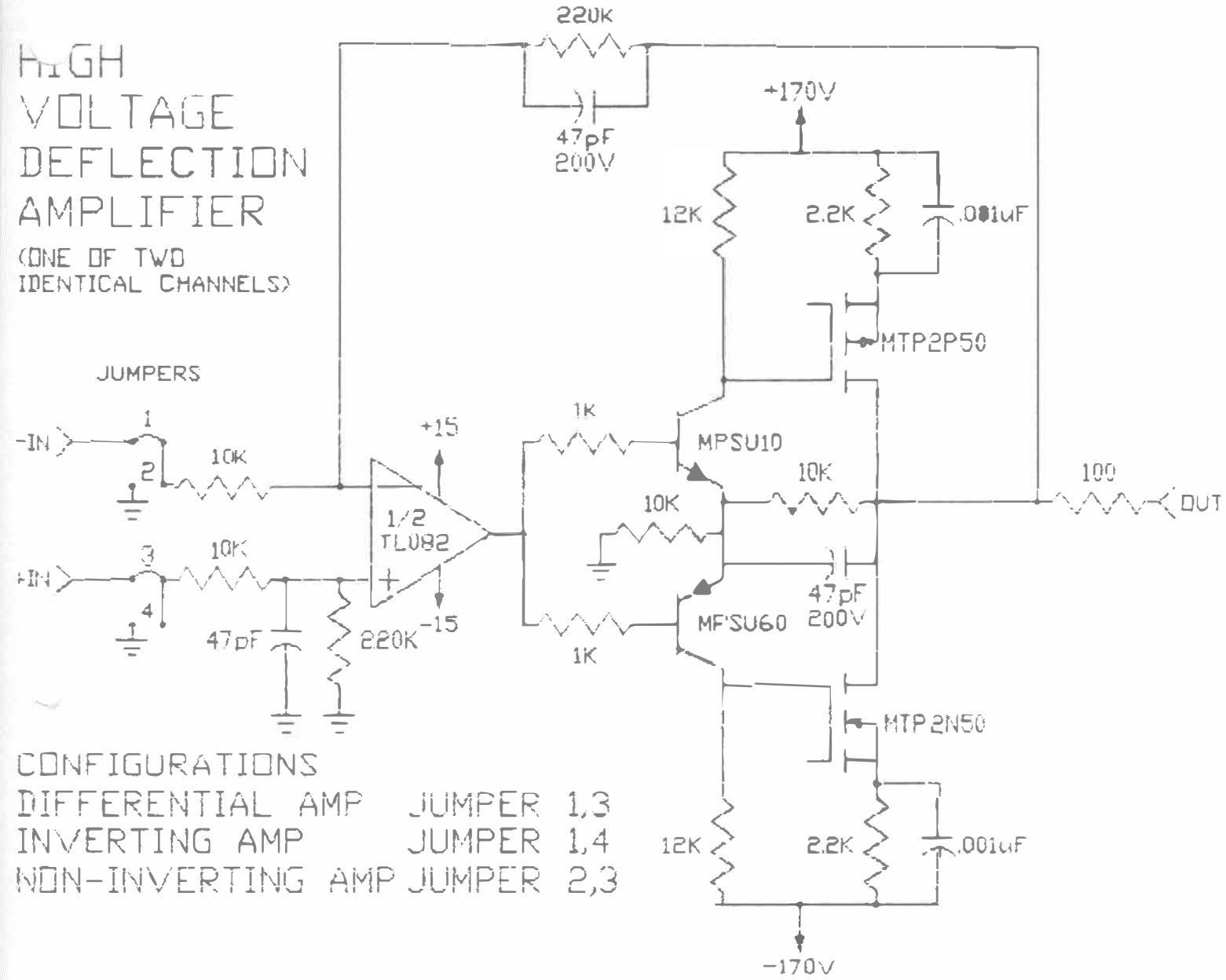

CONFIGURATIONS

DIFFERENTIAL AMP	JUMPER 1,3
INVERTING AMP	JUMPER 1,4
NON-INVERTING AMP	JUMPER 2,3

FIG. 4

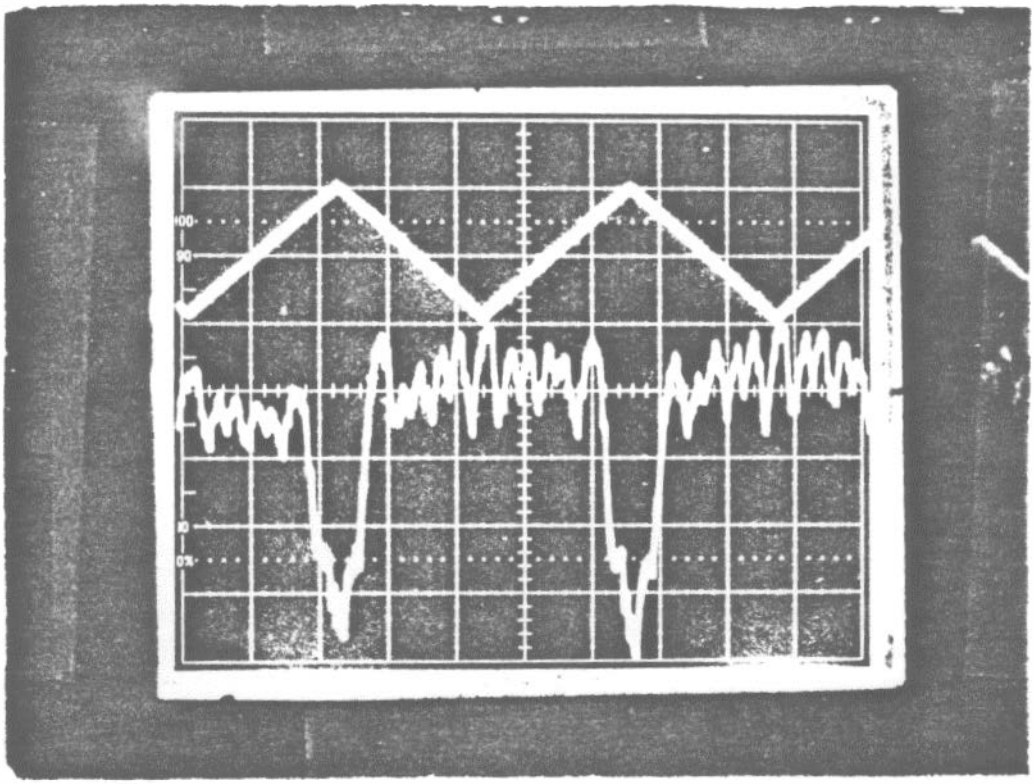

Fig. 3

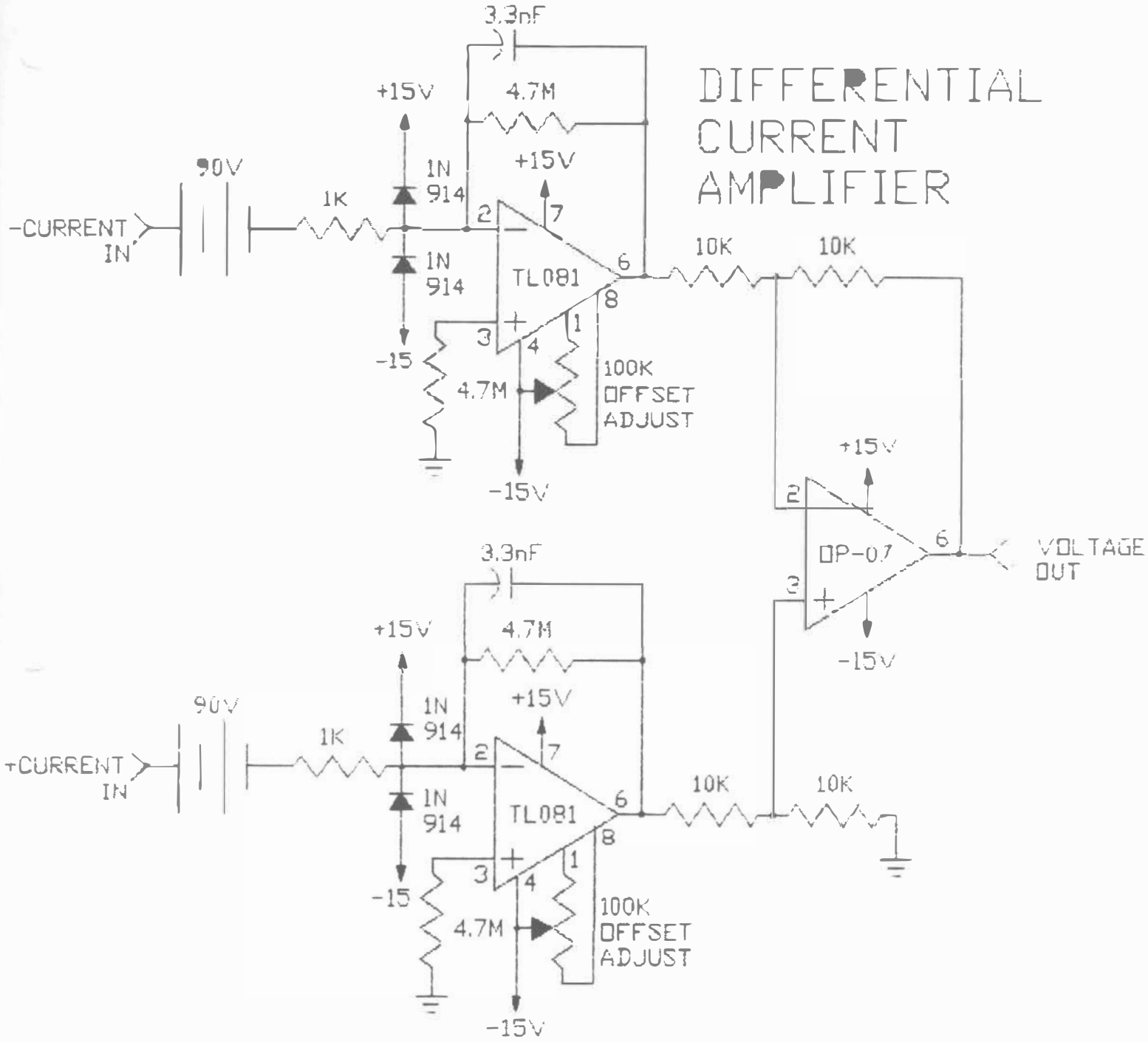
DIFFERENTIAL
CURRENT
AMPLIFIER
3.3nF
4.7M
+15V
90V
1K
1N
914
-CURRENT
IN
TL081
10K
10K
100K
OFFSET
ADJUST
-15
-15V
OP-07
VOLTAGE
OUT
+CURRENT
IN

FIG. 6

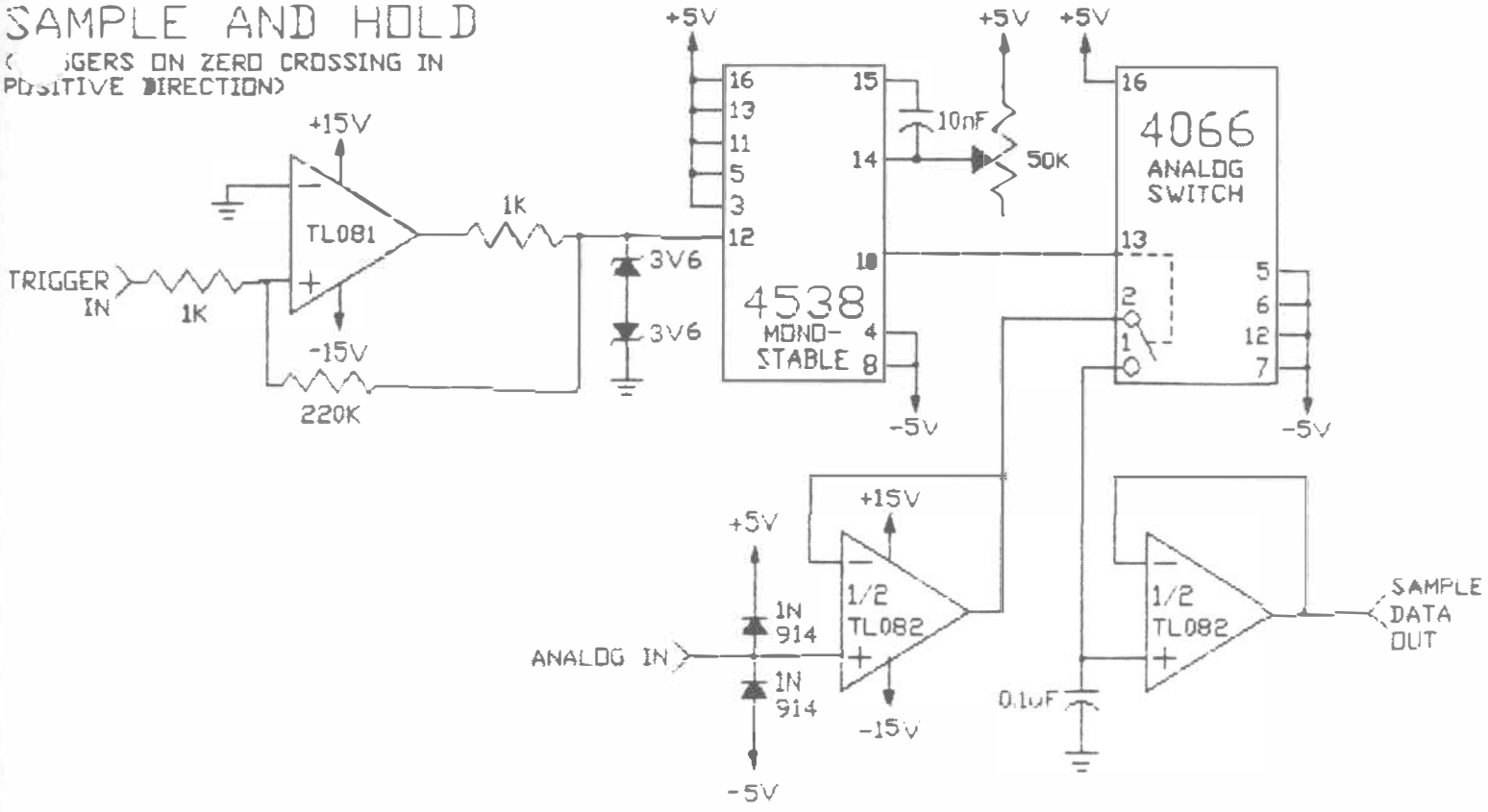
SAMPLE AND HOLD
( )GERS ON ZERO CROSSING IN
POSITIVE DIRECTION)
+15V
TL081
TRIGGER
IN
1K
1K
-15V
220K
3V6
3V6
+5V
16
13
11
5
3
12
15
14
10nF
50K
4538
MONO-
STABLE
4
8
-5V
+5V
+5V
16
4066
ANALOG
SWITCH
13
2
1
5
6
12
7
-5V
+5V
+15V
1N
914
1N
914
ANALOG IN
1/2
TL082
-15V
-5V
0.1uF
1/2
TL082
SAMPLE
DATA
OUT

FIG. 7

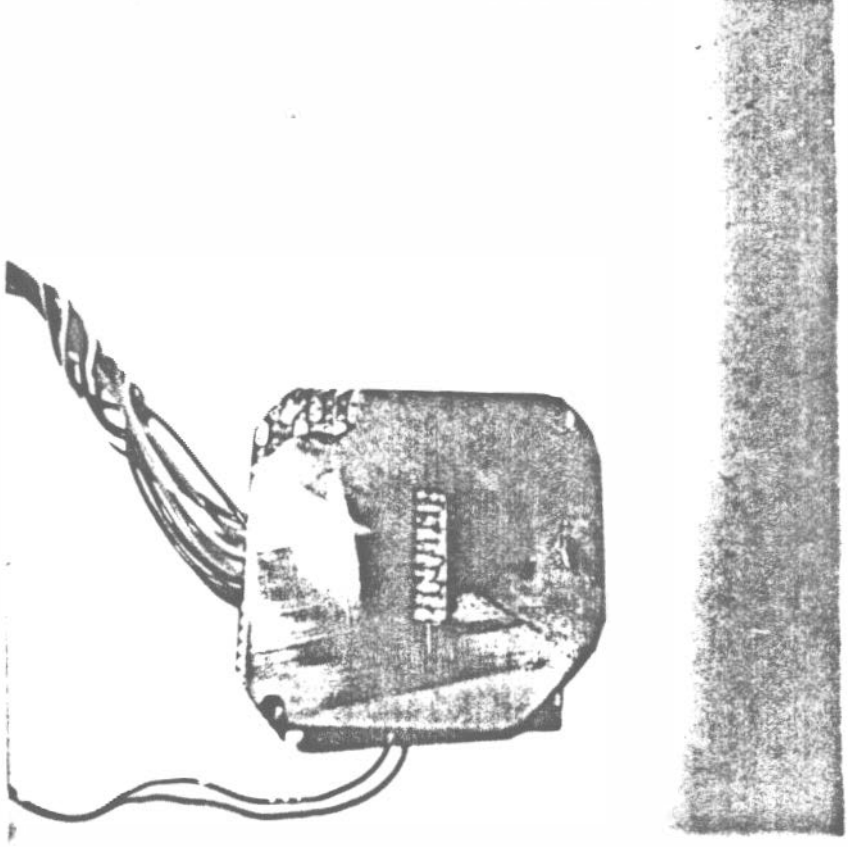

Fig. 8

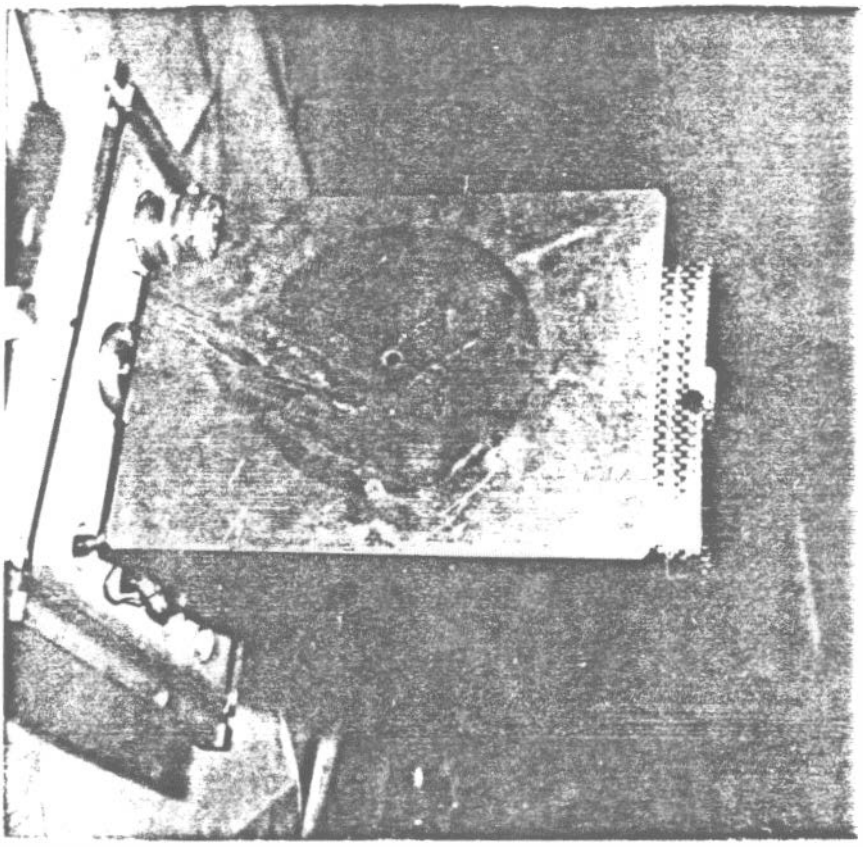

Fig. 9

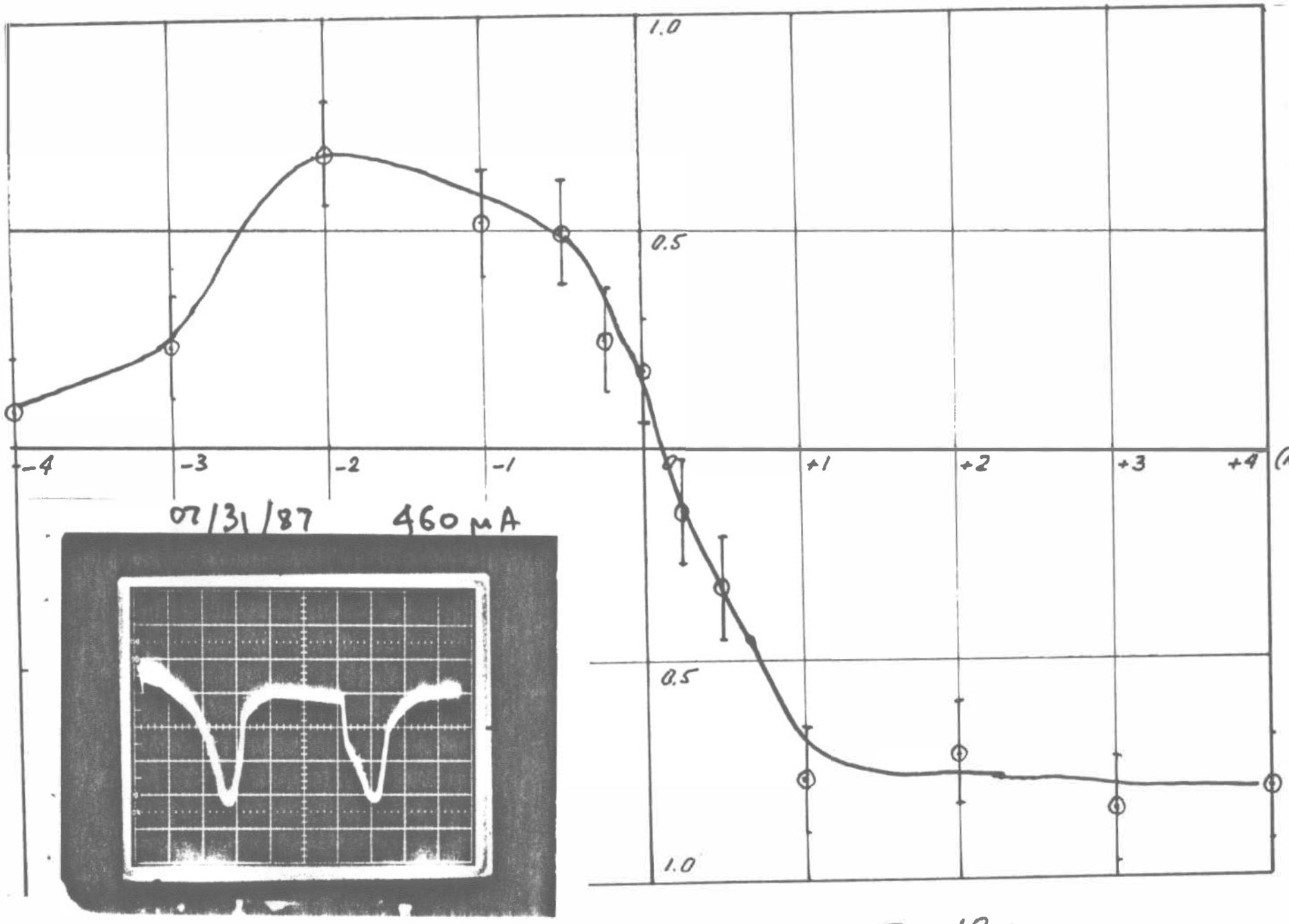

FIG. 10 a

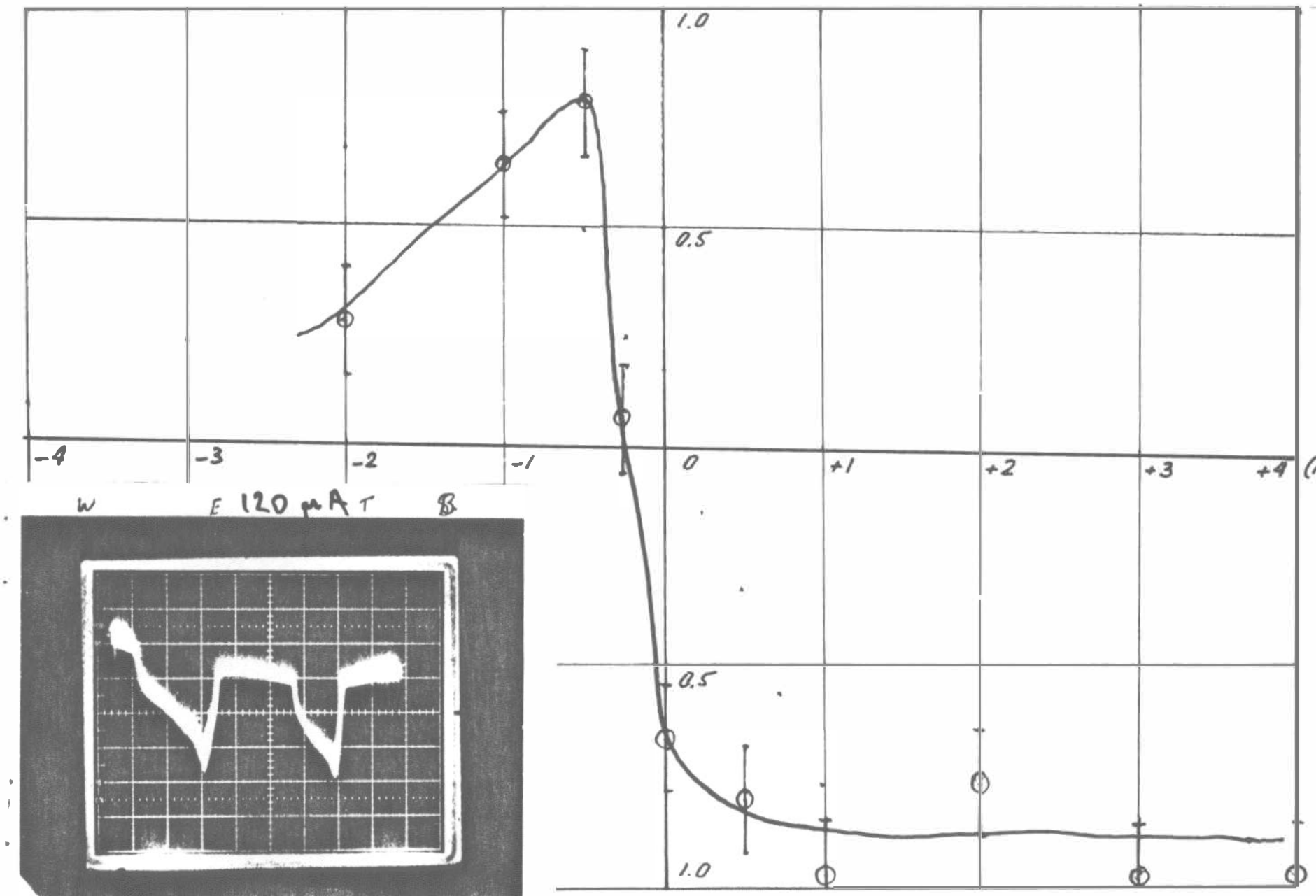

FIG. 10 B

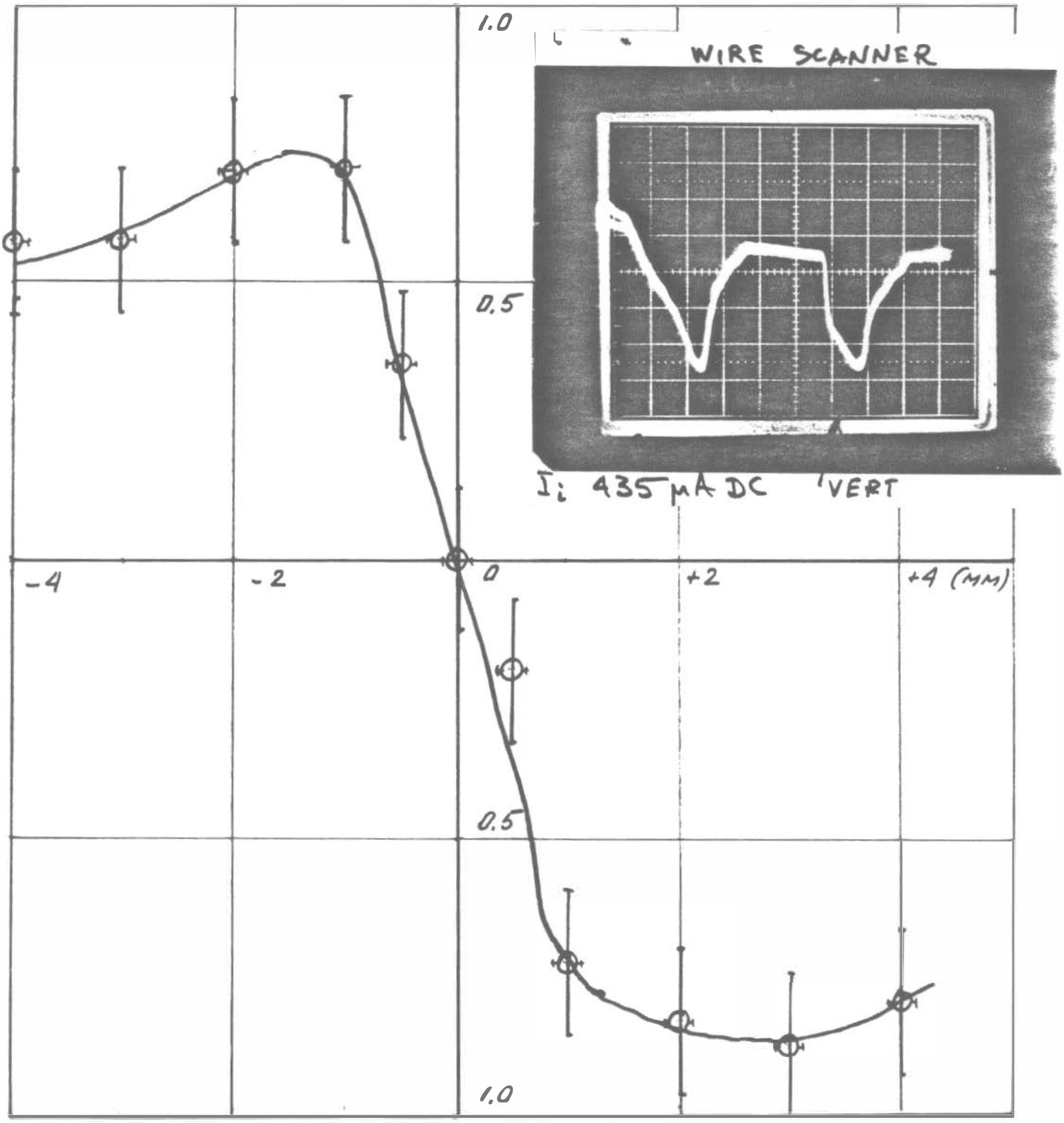

FIG. 10 C

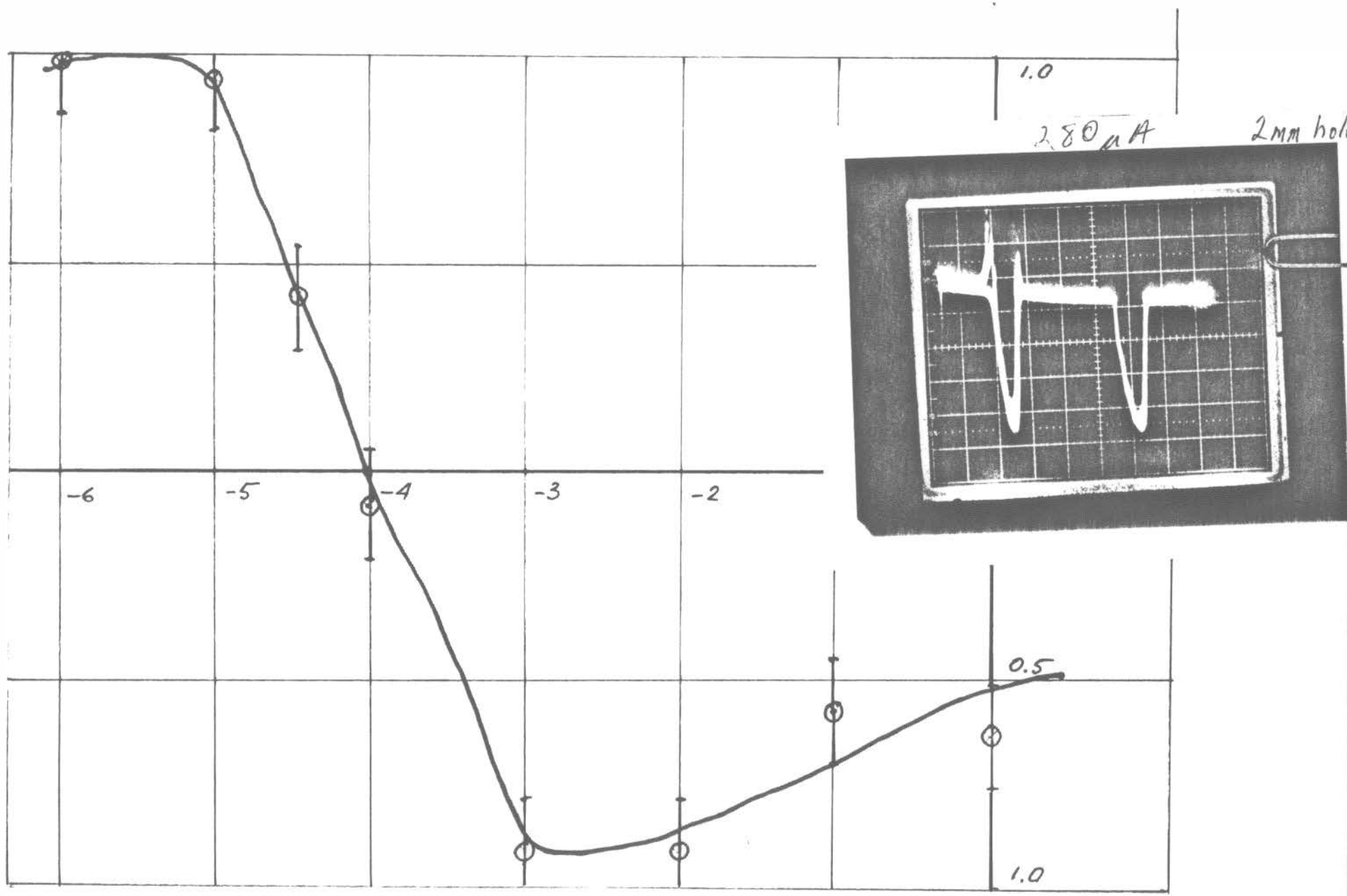

FIG. 10 d

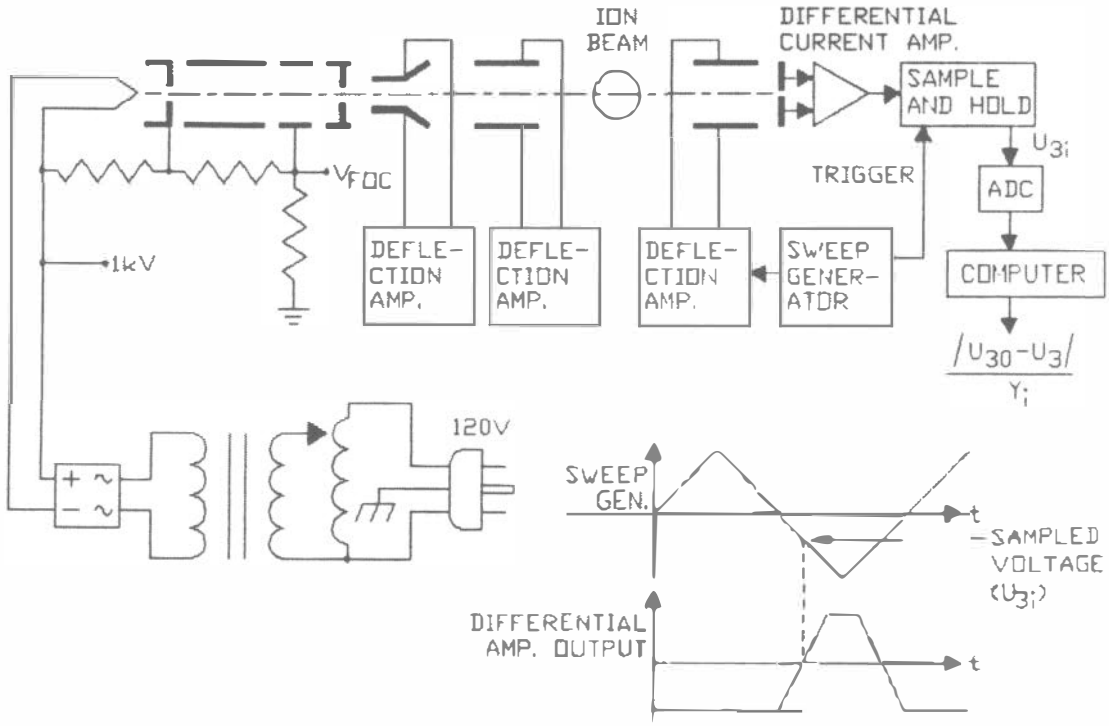
ION
BEAM
DIFFERENTIAL
CURRENT AMP.
SAMPLE
AND HOLD
U_{3i}
TRIGGER
ADC
COMPUTER
$\frac{|U_{30}-U_3|}{Y_i}$
V_{FOC}
1kV
DEFLE-
CTION
AMP.
DEFLE-
CTION
AMP.
DEFLE-
CTION
AMP.
SWEEP
GENER-
ATOR
120V
SWEEP
GEN.
t
SAMPLED
VOLTAGE
(U_{3i})
DIFFERENTIAL
AMP. OUTPUT
t

Fig. 11